NANO MICRO small

Supporting Information

for *Small,* DOI: 10.1002/smll.202205855

Ni Single Atoms on MoS_2 Nanosheets Enabling Enhanced Kinetics of Li-S Batteries

Chenxu Dong, Cheng Zhou, Yan Li, Yongkun Yu, Tianhao Zhao, Ge Zhang, Xinhui Chen, Kaijian Yan, Liqiang Mai, and Xu Xu**

Supporting Information

Ni single atom on MoS_2 nanosheets enabling enhanced kinetics of Li-S batteries

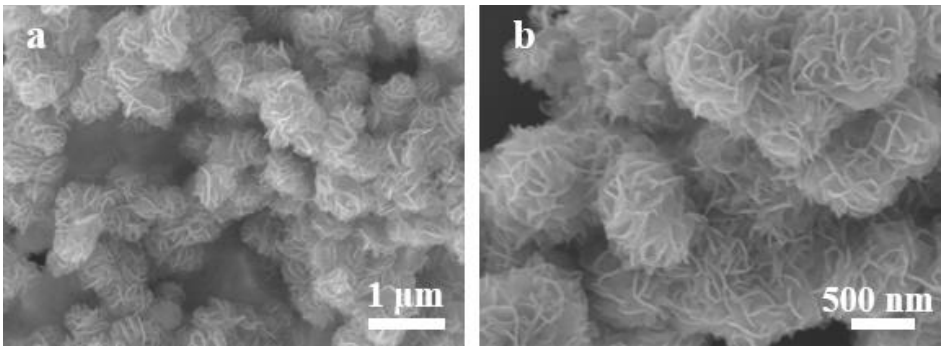

Figure S1. (a-b) The SEM images of Ni-MoS_2 nanosheets.

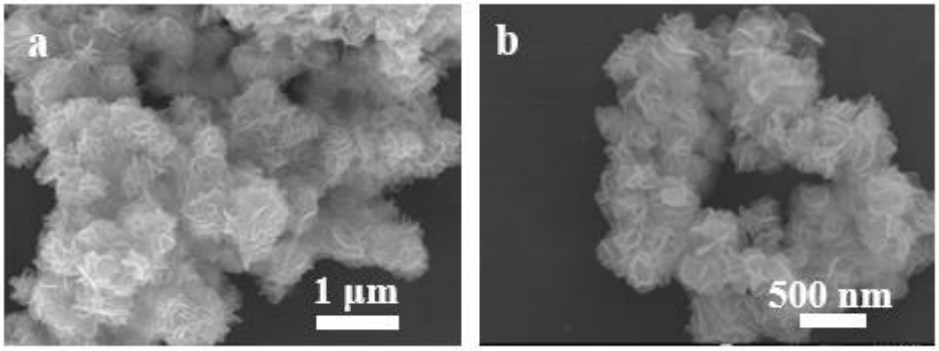

Figure S2. (a-b) The SEM images of MoS_2 nanosheets.

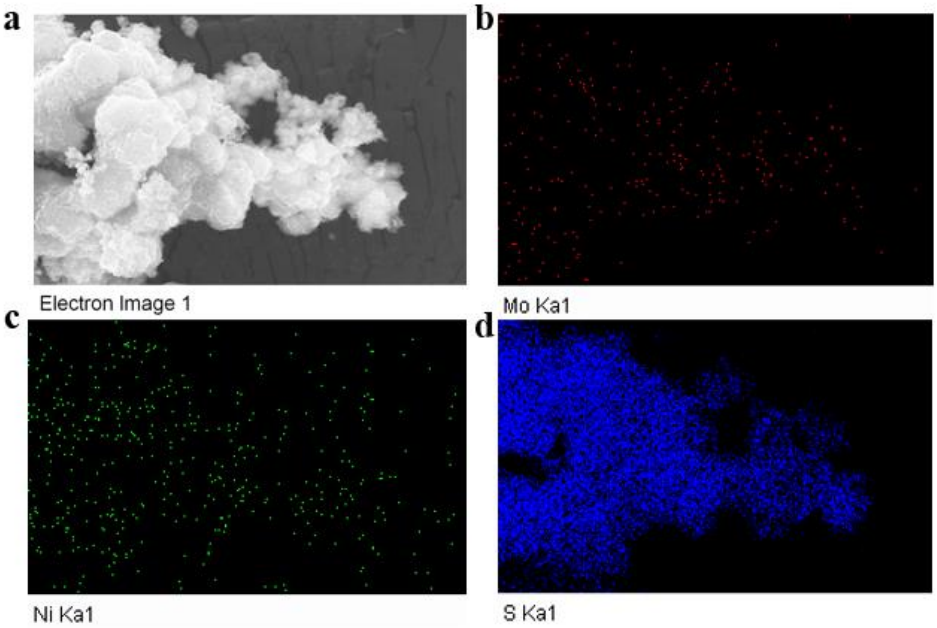

Figure S3. The elemental mappings of Ni-MoS_2 nanosheets.

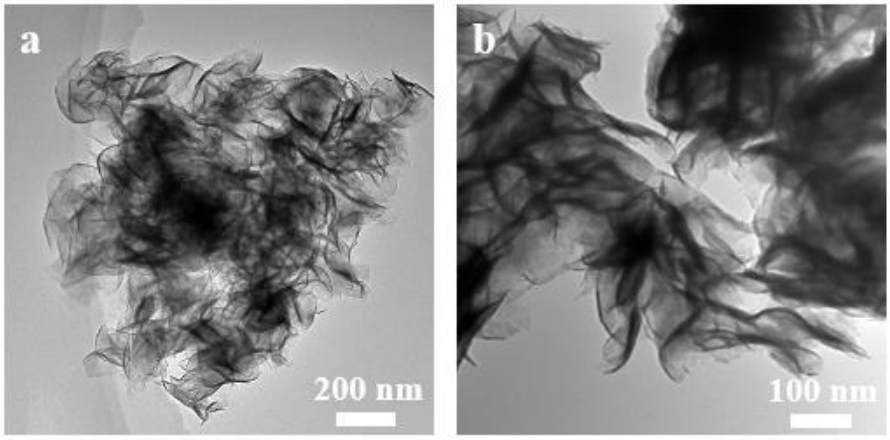

Figure S4. (a-b) The TEM images of MoS_2 nanosheets.

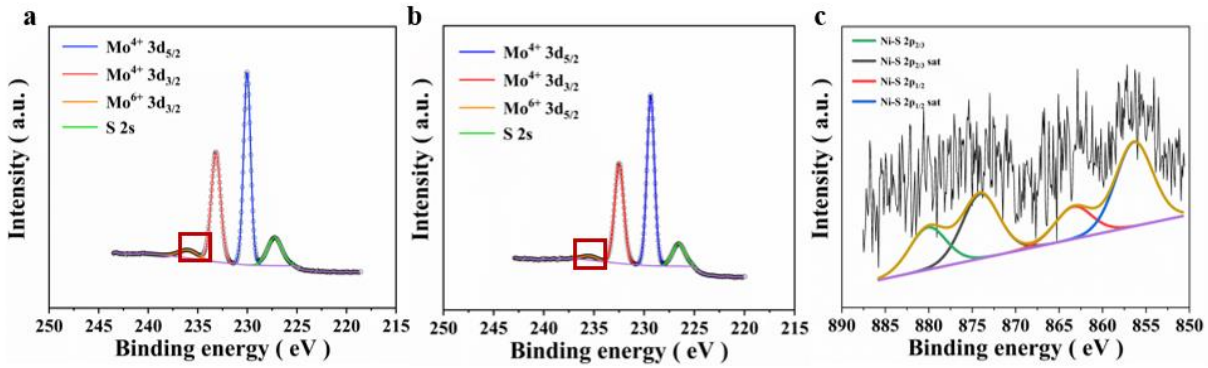

Figure S5. The XPS spectra of MoS_2, Ni-MoS_2: (a) Mo 3d spectra of Ni-MoS_2, as well as (b) Mo 3d spectra of MoS_2 and (c) Ni 2p spectra.

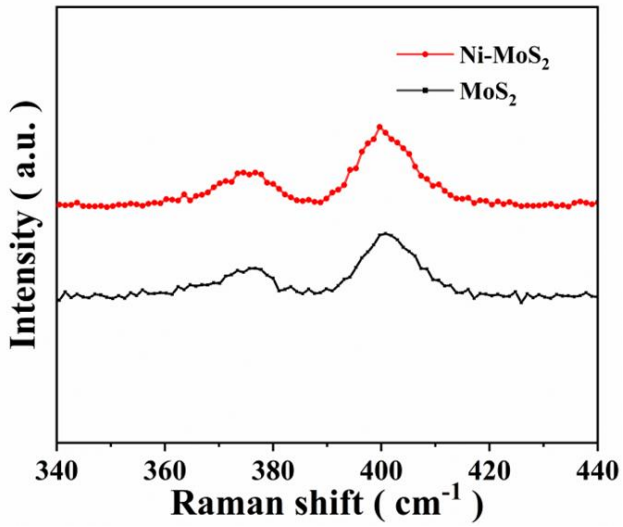

Figure S6. Raman spectra of the Ni-MoS_2 nanosheets and MoS_2 nanosheets.

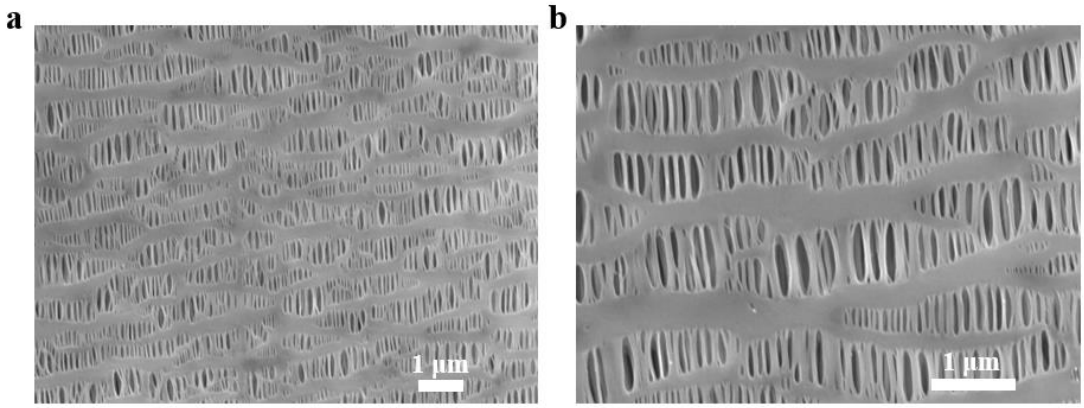

Figure S7. (a-b) The SEM images of the surface of pristine PP separator.

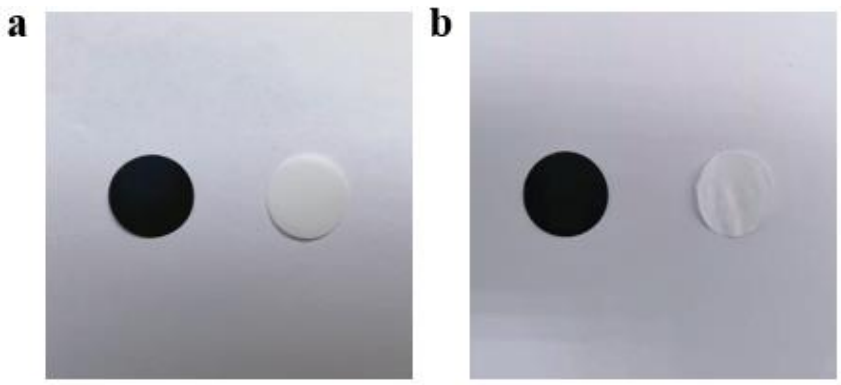

Figure S8. Digital photographs of the Ni-MoS_2@PP separator (on the left) and PP separator (on the right) before and after 120°C for 24h.

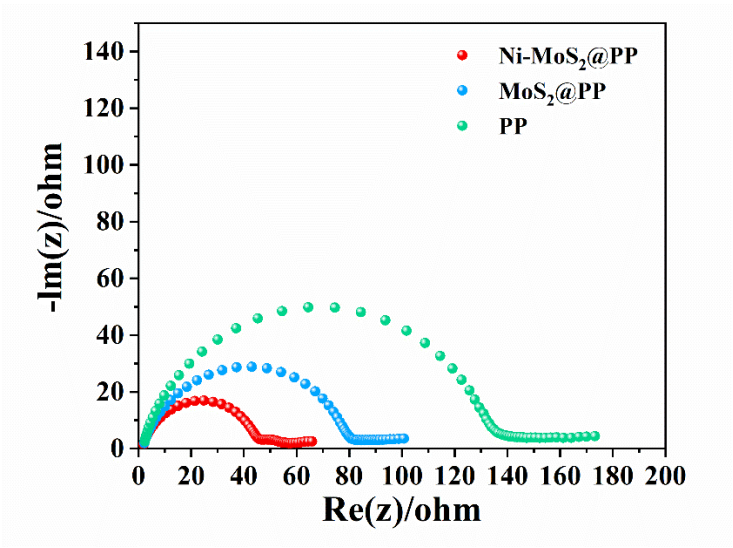

Figure S9. The electrochemical impedance spectroscopic (EIS) spectra of symmetric batteries assembled with different separators.

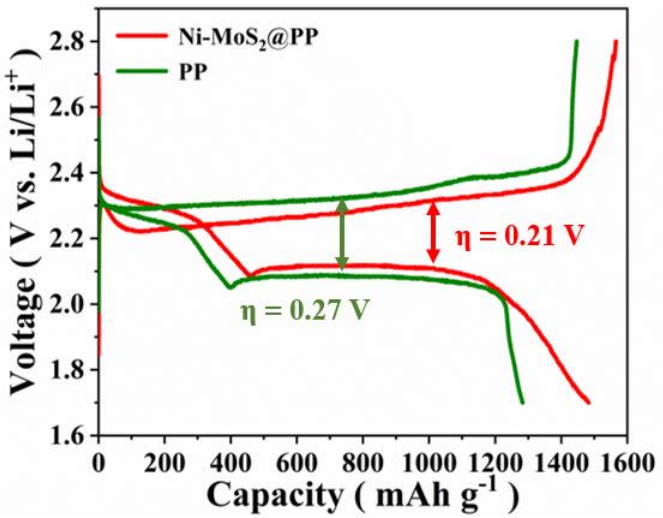

Figure S10. Galvanostatic charging/discharging performance of Li-S batteries with different separators at 0.2 C.

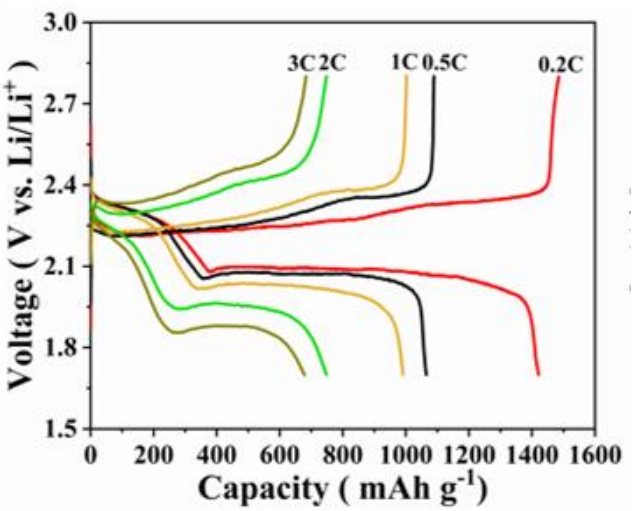

Figure S11. Galvanostatic charge-discharge profiles of the Li-S batteries with Ni-MoS_2@PP separator at different rates in a potential window from 1.7 to 2.8V.

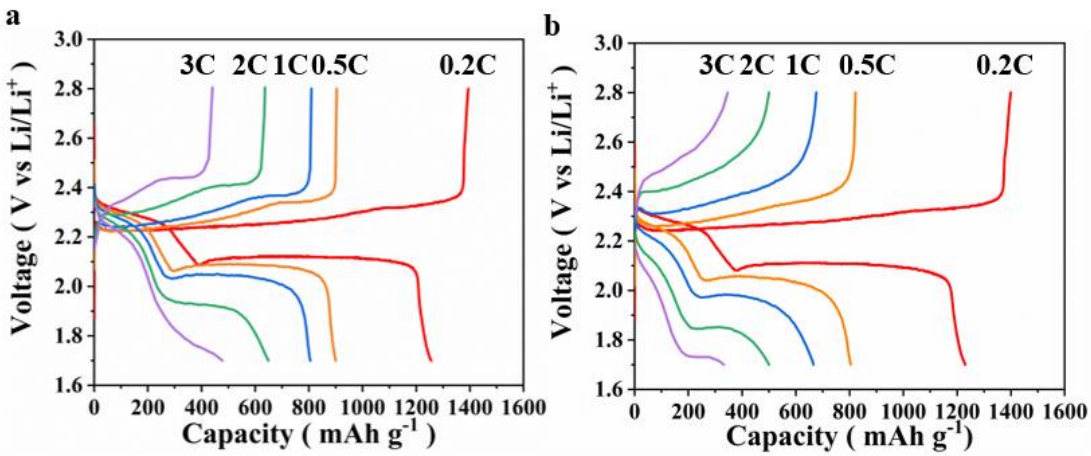

Figure S12. Galvanostatic charge-discharge profiles of the Li-S batteries with (a) MoS_2@PP separator and (b) PP separator at different rates in a potential window from 1.7 to 2.8V.

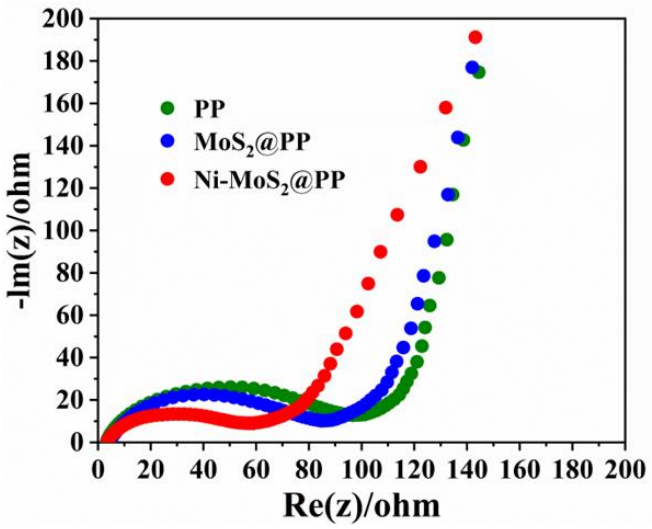

Figure S13. The electrochemical impedance spectroscopic (EIS) spectra of Li-S battery assembled with different separators.

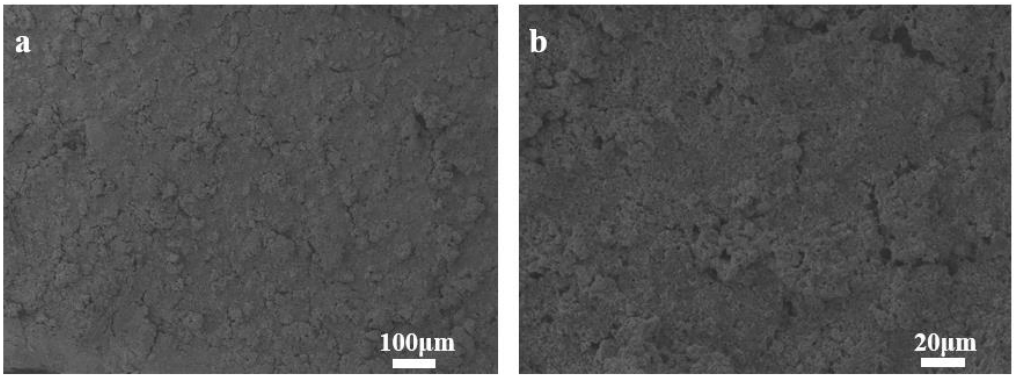

Figure S14. (a-b) SEM images of the surface of Ni-MoS_2@PP after 20 cycles.

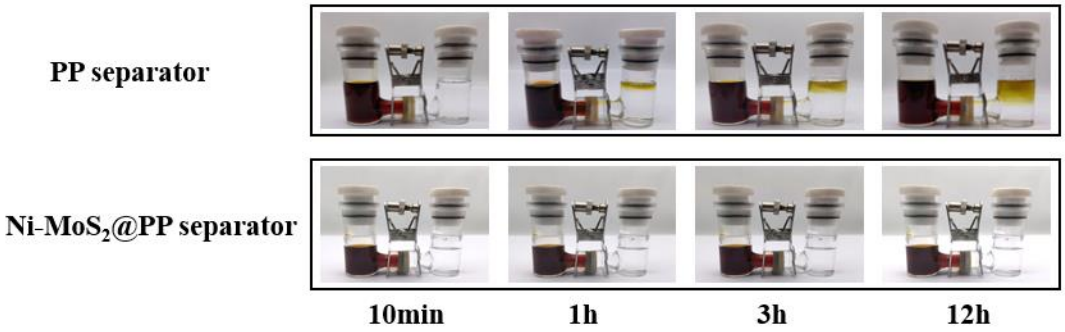

Figure S15. Shuttling tests with a double-L device for the Ni-MoS_2@PP separator and the pristine PP separator.

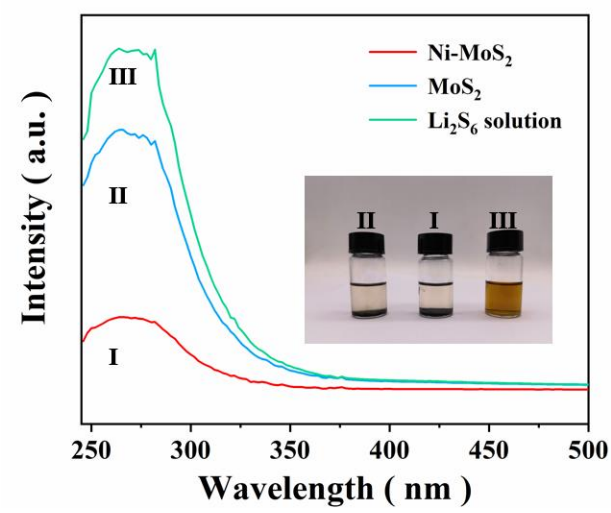

Figure S16. UV-vis spectra of the Li_2S_6 solution mixed with different samples, the inset is the photograph of sealed vials after adsorption.

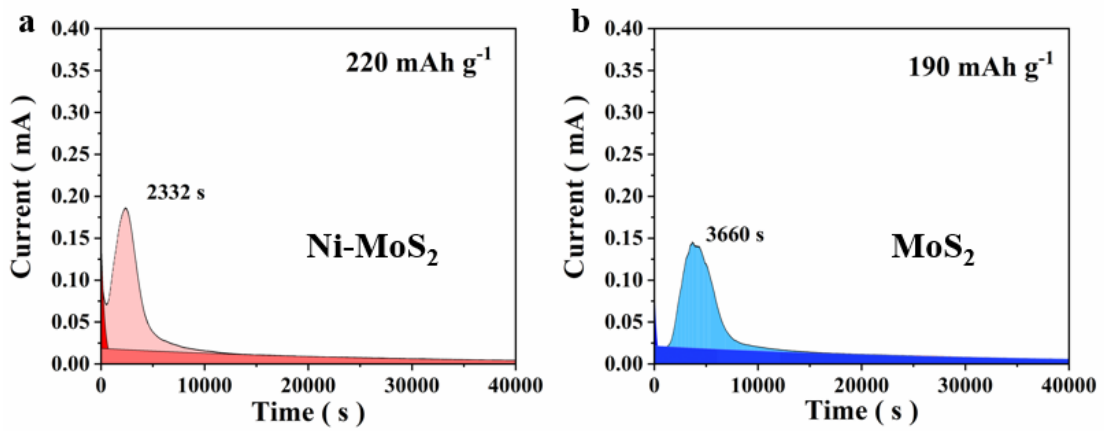

Figure S17. Potentiostatic discharge profiles of Li_2S_6 solution at 2.05 V for the nucleation and dissolution of Li_2S on the Ni-MoS_2 and MoS_2 electrodes.

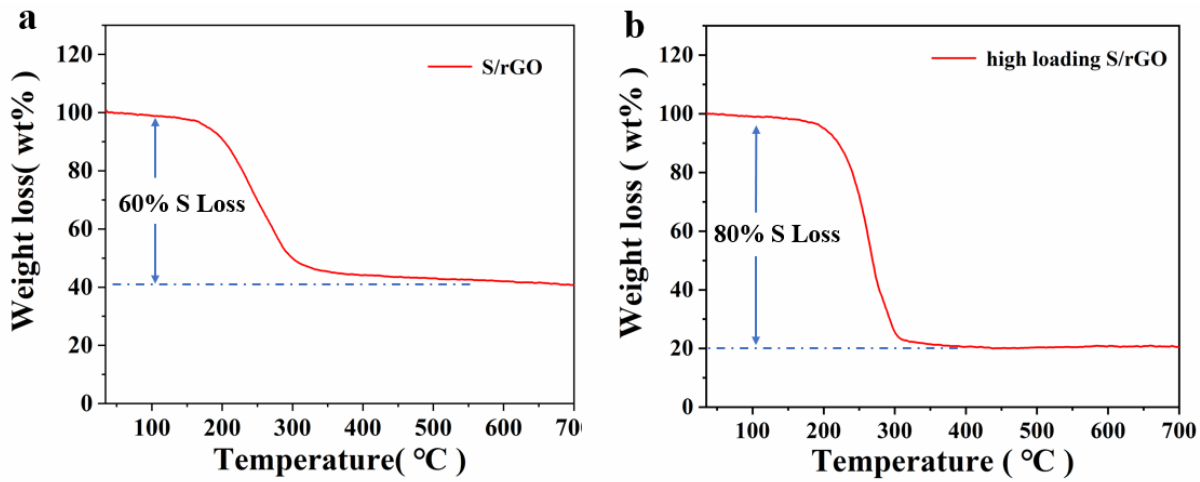

Figure S18. TGA curve of sulfur content with normal sulfur loading (a) and high sulfur loandig (b).

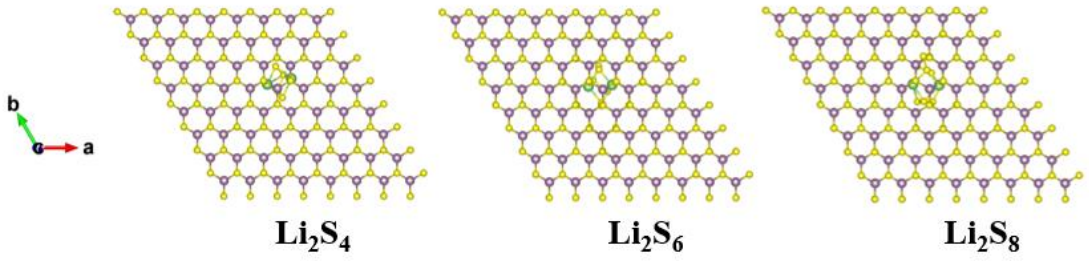

Figure S19. Top view of the optimized configurations for the binding of long-chain Li_2S_n to MoS_2.

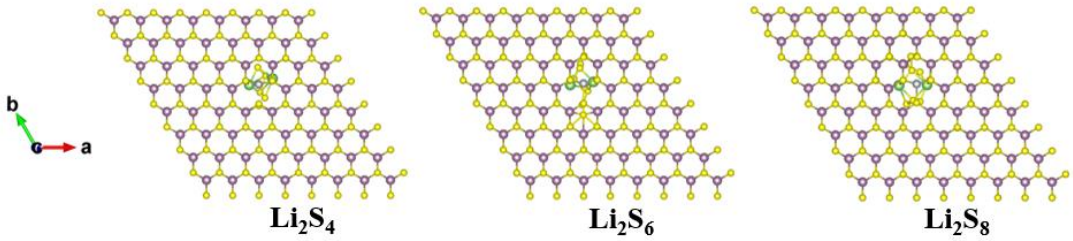

Figure S20. Top view of the optimized configurations for the binding of long-chain Li_2S_n to Ni-MoS_2.

Table S1. Detailed information of Li-S batteries fabricated with metal sulfide/single atom modified separators.

Metal sulfide / Single atom	Areal sulfur loading (mg cm^{-2})	High sulfur loading (mg cm^{-2})	Maximum capacity (mAh g^{-1})	Rate capacity (mAh g^{-1})	Fading rate (%)		Ref.
					Low rate	High rate	
W/NG	1.1	8.3	1389 (0.2 C)	678 (10 C)	0.10 (0.5 C)	0.05 (2 C)	[1]
Co_9S_8	2	5.6	1385 (0.1 C)	428 (2 C)	0.07 (0.1 C)	0.01 (1 C)	[2]
COS_2/NSCNHF@C	1.2	2.04	1284.5 (0.1 C)	522 (2 C)	0.48 (0.5 C)	0.20 (1 C)	[3]
CNF/CoS/KB	1.8	-	1500 (0.1 C)	650 (2 C)	0.12 (0.5 C)	0.08 (1 C)	[4]
CoS@g-C_3N_4	1.5	4	1290 (0.2 C)	690 (2 C)	0.08 (0.5 C)	0.03 (1 C)	[5]
Co_9S_8/CoO	1	2.5	1201 (0.02 C)	536 (5 C)	-	0.05 (1 C)	[6]
B/2D MOF-Co	1.5	7.8	1112 (0.1 C)	478 (5 C)	0.13 (0.5 C)	0.07 (1 C)	[7]
Mn-N-C	1.2	4.91	1596 (0.1 C)	581 (2 C)	0.05 (0.5 C)	0.05 (1 C)	[8]
NiS_2	1	-	1515 (0.2 C)	801 (2 C)	0.07 (0.5 C)	0.07 (2 C)	[9]
Fe@NG	1.1	-	1616 (0.1 C)	820 (2 C)	0.07 (0.2 C)	0.02 (2 C)	[10]
MoS_2	-	-	1471 (0.1 C)	550 (1 C)	0.08 (0.5 C)	-	[11]
MoS_2/graphene	0.8-1.2	-	1642 (0.12 C)	600 (5 C)	0.56 (0.12 C)	0.13 (1.2 C)	[12]
Ni-MoS_2	2.5	7.5	1329 (0.2 C)	677 (3 C)	0.15 (0.5 C)	0.01 (2 C)	This work

Reference

[1] Wang, P.; Xi, B.; Zhang, Z.; Huang, M.; Feng, J.; Xiong, S. Atomic Tungsten on Graphene with Unique

Coordination Enabling Kinetically Boosted Lithium–Sulfur Batteries. *Angew. Chem. Int. Ed.* **2021**, 60, 15563-15571.

[2] He, J.; Chen, Y.; Manthiram, A. Vertical Co_9S_8 hollow nanowall arrays grown on a Celgard separator as a multifunctional polysulfide barrier for high-performance Li–S batteries. *Energy Environ. Sci.* **2018**, 11, 2560-2568.

[3] Wang, J.; Cai, W.; Mu, X.; Han, L.; Wu, N.; Liao, C.; Kan, Y.; Hu, Y. Designing of multifunctional and flame retardant separator towards safer high-performance lithium-sulfur batteries. *Nano Res.* **2021**, 14, 4865-4877.

[4] Yang, Y.; Wang, S.; Zhang, L.; Deng, Y.; Xu, H.; Qin, X.; Chen, G. CoS-interposed and Ketjen black-embedded carbon nanofiber framework as a separator modulation for high performance Li-S batteries. *Chem. Eng. J.* **2019**, 369, 77-86.

[5] Liu, X.; Wang, S.; Duan, H.; Deng, Y.; Chen, G. A thin and multifunctional CoS@g-C_3N_4/Ketjen black interlayer deposited on polypropylene separator for boosting the performance of lithium-sulfur batteries. *J. Colloid Interface Sci.* **2022**, 608, 470-481.

[6] Wang, N.; Chen, B.; Qin, K.; Liu, E.; Shi, C.; He, C.; Zhao, N. Rational design of Co_9S_8/CoO heterostructures with well-defined interfaces for lithium sulfur batteries: A study of synergistic adsorption-electrocatalysis function. *Nano Energy*. **2019**, 60, 332-339.

[7] Li, Y.; Lin, S.; Wang, D.; Gao, T.; Song, J.; Zhou, P.; Xu, Z.; Yang, Z.; Xiao, N.; Guo, S. Single Atom Array Mimic on Ultrathin MOF Nanosheets Boosts the Safety and Life of Lithium–Sulfur Batteries. *Adv. Mater.* **2020**, 32, 1906722.

[8] Qiao, S.; Lei, D.; Wang, Q.; Shi, X.; Zhang, Q.; Huang, C.; Liu, A.; He, G.; Zhang, F. Etch-evaporation enabled defect engineering to prepare high-loading Mn single atom catalyst for Li-S battery applications. *Chem. Eng. J.* **2022**, 442, 136258.

[9] Wang, J.; Xu, J.; Tang, W.; Niu, D.; Zhao, S.; Hu, S.; Zhang, X. Infixing NiS_2 nanospheres into a three-dimensional rGO/CNTs-Li carbon composite as superior electrocatalyst for high-performance Li-S batteries. *ChemNanoMat*. **2020**, 6, 976-983.

[10] Cao, G.; Wang, Z.; Bi, D.; Zheng, J.; Lai, Q.; Liang, Y. Atomic-Scale Dispersed Fe-Based Catalysts Confined on Nitrogen-Doped Graphene for Li-S Batteries: Polysulfides with Enhanced Conversion Efficiency. *Chem. – Eur. J.* **2020**, 26, 10314-10320.

[11] Ghazi, Z. A.; He, X.; Khattak, A. M.; Khan, N. A.; Liang, B.; Iqbal, A.; Wang, J.; Sin, H.; Li, L.; Tang, Z. MoS_2 / Celgard Separator as Efficient Polysulfide Barrier for Long-Life Lithium-Sulfur Batteries. *Adv. Mater.* **2017**, 29, 1606817.

[12] Guo, P.; Liu, D.; Liu, Z.; Shang, X.; Liu, Q.; He, D. Dual functional MoS_2/graphene interlayer as an efficient polysulfide barrier for advanced lithium-sulfur batteries. *Electrochimica Acta*. **2017**, 256, 28-36.